INEEL/EXT-01-01225

Dissolution Kinetics of Alumina Calcine

T. A. Batcheller
T. G. Garn
D. R. Peterman

September 2001

Idaho National Engineering and Environmental Laboratory
Bechtel BWXT Idaho, LLC

INEEL/EXT-01-01225

Dissolution Kinetics of Alumina Calcine

T. A. Batcheller
T. G. Garn
D. R. Peterman

September 2001

Idaho National Engineering and Environmental Laboratory
Idaho Falls, Idaho 83415

Prepared for the
U.S. Department of Energy
Assistant Secretary for Environmental Management
Under DOE Idaho Operations Office
Contract DE-AC07-99ID13727

SUMMARY

Dissolution kinetics of alumina type non-radioactive calcine was investigated as part of ongoing research that addresses permanent disposal of Idaho High Level Waste (HLW). Calcine waste was produced from the processing of nuclear fuel at the Idaho Nuclear Technology and Engineering Center (INTEC). Acidic radioactive raffinates were solidified at ~500ºC in a fluidized bed reactor to form the dry granular calcine material. Several Waste Management alternatives for the calcine are presented in the Idaho High Level Waste Draft EIS. The Separations Alternative addresses the processing of the calcine so that the HLW is ready for removal to a national geological repository by the year 2035. Calcine dissolution is the key front-end unit operation for the separations alternative.

Because aluminum and zirconium-type fuels were predominately reprocessed at the INTEC, alumina and zirconia-type calcines were produced and stored. Dissolution kinetics testing with non-radioactive pilot plant zirconia calcine has been previously investigated. Similar to that work, the scope of this present alumina calcine dissolution work included: 1) chemical and physical analyses of the calcine material, 2) baseline dissolution testing to determine: order of reaction, activation energy (Arrhenius analysis), and dissolution rate controlling mechanism (chemical reaction or mass transfer limited). Testing was also performed to determine if complete dissolution is equilibrium/solubility inhibited.

Chemical and physical analyses were performed on the RSH-1 alumina type pilot plant calcine bed material. Elemental fusion analysis results agree well with microprobe analysis results. An average value of the calcine acid consumption coefficient, **b**, was determined for RSH-1 bed product material; **b** = 19.8 grams RSH-1 dissolved per mol of acid consumed. The *order of reaction* testing revealed that, just as in the case for the Run74 zirconia pilot plant calcine testing, the homogeneous rate form fit the rate data better than the heterogeneous rate form. A characteristic *dissolution fractal dimension*, D_R, was determined for alumina and zirconia pilot plant calcine milled material and bed particles. The result from this fractal treatment of the dissolution data further supports the indication that calcine dissolution is more dependent upon its physical characteristics, rather than its chemical characteristics. Arrhenius testing yielded an *apparent activation energy* (E_A) of 26.9 kcal/mol for RSH-1 alumina pilot plant calcine under conditions of constant 6 M acid concentration. The *dissolution rate controlling* mechanism testing results were inconclusive. Nevertheless, it was noted that, just as with all previous calcine dissolution testing, this testing with RSH-1 showed the familiar initial rapid dissolution then the leveling-out of the rate, and the non-attainment of 100% dissolution after long dissolution times—it too had the characteristics of internal mass diffusion controlled dissolution. The equilibrium/solubility inhibition testing results indicated that, the slowing dissolution rate of alumina compounds was preventing complete dissolution, and the data did not suggest that complete dissolution of RSH-1 calcine was equilibrium/solubility inhibited. The greatest percent mass dissolution observed during this testing with RSH-1 was 93.0 %; this was achieved after eight hours of dissolution at 95ºC.

ACKNOWLEDGEMENTS

The authors wish to take this opportunity to thank Mr. Arlin Olson and Dr. R. Scott Herbst for their expert review and input. Thanks to Messrs. Mike Phippen and Wade Waddoups (machine shop), and Gary Gregston (glass shop) for providing special laboratory equipment fabrication services. Thanks to Mr. Wes Gamett for his invaluable help with the laboratory work. Thanks to Ms. Karen Wright for her microprobe analysis work. And finally, thanks to the INTEC analytical department for their accurate and expeditious sample result reporting. Without the work ethic and dedication of these employees, this work would never have been accomplished.

CONTENTS

FIGURES

TABLES

Dissolution Kinetics of Alumina Calcine

1. INTRODUCTION

Nuclear fuels were reprocessed at the Idaho Nuclear Technology Engineering Center (INTEC) (formerly the Idaho Chemical Processing Plant) located at the Idaho National Engineering and Environmental Laboratory (INEEL) for about 35 years. These were predominately aluminum and zirconium type fuels. They were dissolved in acidic aqueous media and the uranium was separated from the radioactive solutions utilizing liquid-liquid extraction processes. The liquid radioactive raffinates were subsequently solidified (calcined) in a fluidized bed reactor to form a dry granular material. Originally calcination was accomplished with an in-bed heat exchanger at 400°C and subsequently (beginning in 1970) at 500°C with in-bed combustion of kerosene. This calcine has been provisionally stored near surface in concrete encased stainless steel bins at the INTEC. The radioactive nuclides constitute only about one weight percent of the calcine; the remainder is non-radioactive fuel matrix and fuel reprocessing material.

Research addressing the permanent immobilization of radioactive waste has been ongoing. Several Waste Management alternatives are presented in the Idaho High Level Waste (HLW) Draft EIS[1]. The Separations Alternative addresses the processing of the calcine so that it is ready for shipment to a national geological repository by the year 2035. Separations reduces the HLW radioactive waste volume to be ultimately stored at the repository. Nitric acid dissolution of the calcine is an essential front-end unit operation in the separations option. In order to design calcine dissolution equipment, a dissolution reaction rate expression is required. Investigation of the dissolution kinetics of an alumina type calcine is presented in this report.

2. BACKGROUND

Pilot plant scale fluidized bed calciners have been utilized since the early 1960's to develop and verify calcination flowsheets for the various radioactive liquid wastes generated at the INTEC. A non-radioactive calcine material is produced in these pilot plant calciners and it is physically and chemically similar to the actual radioactive calcine. Typically, dissolution of the pilot plant calcine is part of the scope of calcination development work. In addition, dissolution studies were performed to support the ongoing operations at the INTEC radioactive waste calcination facilities[2,3]. These studies have traditionally been qualitative in nature, most resulting in a "snapshot" of the dissolution (usually after an hour of dissolution time), and a dissolution rate expression for a calcine dissolver design was not addressed. The dissolution kinetics and dynamics of a zirconia-type pilot plant calcine (designated as Run74) was previously investigated[4]. This work primarily used mass conversion and coupled in-dissolution particle size distribution (psd) data to develop an expression for the rate of dissolution. This dissolution model was fairly constrained. The data indicated that calcine dissolution was controlled by pore diffusion inside the particle.

During his work with calcine, Herbst realized an adequately representative alumina pilot plant calcine was not available[5]. Of primary concern was a representative boron and mercury content. Mercury was used as a catalyst during dissolution of aluminum-clad fuel, and boron was added to enhance formation of the more soluble amorphous phase alumina during the calcination process. Based on this, the Applied Technology 10-cm pilot plant calciner was utilized to produce a representative alumina calcine surrogate. Approximately 30 lbs. of alumina type calcine was produced in December of 1998, and was designated as "RSH-1". The study of the dissolution kinetics of this calcine is presented in this report.

The scope of the dissolution kinetics testing performed with the RSH-1 alumina pilot plant calcine included: 1) chemical and physical analyses, 2) baseline dissolution testing to determine: *order of reaction*, activation energy (Arrhenius analysis), and dissolution rate controlling mechanism (chemical reaction or mass transfer limited). Testing was also performed to determine if complete dissolution is equilibrium/solubility inhibited.

3. EXPERIMENTAL

3.1 Chemical and Physical Analyses of RSH-1 Alumina Calcine

To determine the chemical composition of RSH-1 calcine material, three types of fusion analysis were performed— lithium tetraborate, sodium hydroxide, and sodium carbonate. These fusion methods are utilized for determining a target set of analytes. Most metals are determined with the lithium tetraborate fusion. Nitrate, chloride, sulfate, and lithium and boron are determined via the sodium hydroxide fusion. The sodium carbonate fusion is used to determine the fluoride and phosphate composition. Fusion analyses were performed on both bed product and the fines material. There were no special sample preparations used prior to the analysis.

Oxygen content in calcine is significant. Since oxygen can not be determined using the fusion analysis methods, an electron microscope was used to obtain wt. % oxygen in RSH-1; several other light elements were also analyzed. A JEOL JXA-8900R Electron Microprobe instrument was utilized for this purpose. Bed product particles were mounted in a small epoxy disk cast. This disk was ground and polished. By this technique, full particle cross sections are available for analysis. Analyses were done for near exterior particle surface locations, and for locations near the center of the particle. Mount preparations were typical; carbon coated mounts were used for all analytes except carbon; aluminum coated mounts were used for determining carbon. In addition to these microprobe analyses, a Scanning Electron Microscope (SEM) was used to obtain photomicrographs, providing some morphological information about this alumina calcine. An R.J. Lee Personal SEM was used. In addition, X-ray diffraction analyses were performed using a Siemans D-5000 X-Ray Diffractometer/Generator.

3.2 Baseline Dissolution Kinetics Testing

3.2.1 Calcine Consumption Coefficient Testing

Testing was performed to determine the acid consumption coefficient (**b**) for RSH-1 alumina type pilot plant calcine. This testing was performed with 2 grams of calcine per 100 mLs of acid, at both 60 and >95°C, and with either 4 M or 6 M nitric acid. Tests were performed for a minimum of 1hour, and up to 7 hours of dissolution time. Testing equipment and methods used for determining **b** were the same as those used in the zirconia calcine kinetics testing[4].

3.2.2 Order of Reaction Testing

Order of reaction testing on RSH-1 was performed to classify the dissolution reaction (homogeneous or heterogeneous) and to determine the order of the dissolution reaction with respect to the acid concentration. This testing was performed with screened bed particle material. This was done to obtain as narrow a particle size material as possible; the average particle size used in this testing was 462µm. Dissolutions were performed at 75ºC under conditions of unchanging acid concentration. The ratio of test calcine mass to volume of acid to accomplish this was calculated using the consumption coefficient **b**. For each acid molarity, tests were performed for 1, 2, 3, 6, and 12 minutes of dissolution time. These data were curvefit to determine the initial rate of dissolution (at time = zero). The dissolver vessel equipment used in this testing is shown in Figure 1.

Figure 1. Dissolution Kinetics Testing Equipment

The calcine was added to the at-temperature acid volume in the dissolver vessel. At the predetermined dissolution time, the dissolving slurry was quickly removed and filtered through a pre-weighed Nalgene 0.45µm cellulose nitrate membrane disposable filter. A filtered liquid sample was obtained and submitted for chemical analysis. The UDS were thoroughly water washed and then dried in a convective oven at 50ºC for 6 hours or longer (overnight). Percent mass dissolution (or mass conversion) was determined from the dried mass remaining on the filter. The experimental parameters used in the order of reaction testing are presented in Table 1.

Table 1. Order of Reaction Testing Parameters

Acid M	0.5	1.0	3.0	6.0	8.0
Avg. Initial Calcine Mass (grams)	0.4154	0.4481	1.201	2.192	1.243
Acid Volume (mLs)	1000	500	400	400	400

3.2.3 Arrhenius Analysis Testing

Arrhenius analysis testing was performed to determine the activation energy for dissolution of RSH-1. Testing was performed under the following conditions: 2.2 grams of starting calcine mass in 400 mLs of well-agitated 6 M nitric acid (unchanging concentration during dissolution) — and dissolved for 1, 2, 3, 6, and 12 minutes. Again, these data were used to determine the initial rate of dissolution. This testing was performed using material with an average particle size of 475µm. This testing was executed in the same manner described above in the order of reaction testing segment — the material was added to the at-temperature acid and then the vessel was removed at the predetermined time and filtered; mass conversion as a function of time was determined from dried filter mass and liquid samples were retrieved and submitted for analysis. This Arrhenius test matrix was performed at dissolution temperatures of 60, 67.5, 75, 85, and 95ºC. A Cole Parmer Polystat Constant Temperature Circulator automatic temperature bath was used to maintain test temperature. This temperature bath setup was used for all baseline kinetics testing.

3.2.4 Dissolution Rate Controlling Mechanism Testing

Testing was performed to determine the *dissolution rate controlling* mechanism. A temperature of 75ºC was used throughout this testing. RSH-1 bed material was screened to obtain as narrow a particle size material as possible (except for the material used in the Arrhenius testing). For smaller particle sizes, the bed material required grinding in a jar mill. The various size ranges of this material is provided in Table 2.

Table 2. Dissolution Rate Controlling Testing Screened Material Sizes

U.S. Standard Size	Particle Size Range (µm)	Avg. Particle Size (µm)	
120-100	125⇗150	137	milled material
60-50	250⇗300	257	
45-30 †	355⇗595	475	Bed particles
30-25	595⇗710	655	
20-18	850⇗1000	925	
† this material used in the Arrhenius testing			

For each narrow particle size range, the mass was uniformly split into predetermined per-dissolution aliquots using a spinning riffler. This same riffling technique was employed for all of the other baseline dissolution kinetics testing described earlier. Mass dissolution was again determined as a function of time. At each given average particle size, dissolutions were performed for 2, 6, 12, 30, and 60 minutes: with an additional test for 7 to 8 hours.

3.2.5 Equilibrium/Solubility Inhibition Testing

Additional tests were performed to determine if complete dissolution is equilibrium/solubility inhibited. These tests were performed with the Arrhenius test conditions

and material, except dissolutions were carried out for 1 to 8 hours. Tests were performed at 75 and 95ºC, and the liquid sample data for these longer time tests were combined with the shorter time test data (the 1, 2, 3, 6, and 12 minute 75 and 95ºC data). The same approximately narrow size range bed material (near 475µm) was used to maintain a consistency between this equilibrium/solubility inhibition testing, the Arrhenius, and the order of reaction testing.

4. RESULTS AND DISCUSSION

4.1 Chemical and Physical Analyses of RSH-1 Alumina Calcine Results

Analytical Laboratory results for the fusion analyses performed on the RSH-1 bed product and fines are presented in Table 3.

Table 3. RSH-1 Fusion Analysis Results

RSH-1 Product Composition		RSH-1 Fines Composition	
Log # 010102-9		Log # 010226-4	
Analyte	**Result (wt%)**	**Analyte**	**Result (wt%)**
Metals		Metals	
Aluminum	4.55451E+01	Aluminum	2.44734E+01
Boron	3.17442E-01	Boron	2.37074E-01
Calcium	3.46267E-01	Calcium	1.62283E-01
Cesium	1.67E-02	Cesium	1.14E+00
Europium	2.63295E-02	Europium	2.75377E-03
Iron	3.73314E-02	Iron	5.94434E-02
Magnesium	1.98911E-01	Magnesium	2.12800E-01
Mercury	4.46E-01	Mercury	7.88E-01
Silicon	2.60212E-02	Silicon	4.61494E-02
Sodium	1.94E+00	Sodium	2.42E+00
Strontium	9.75915E-03	Strontium	2.27898E-03
Anions		Anions	
Analyte	**Result (mg/g)**	**Analyte**	**Result (mg/g)**
Chloride	4.3713E-01	Chloride	2.7379E+00
Nitrate	6.44422E+01	Nitrate	8.3974E+01

For these fusion results, there was a notable wt% difference between the bed product and fines results for aluminum, cesium and chloride. The bed product total wt% was approximately 17 wt% more than the fines, with the greatest difference attributed to aluminum.

Microprobe results for the RSH-1 bed particles of average diameter size 275μm are presented in Figure 2. Microprobe results for the ~475μm size bed material, and RSH-1 fines material are presented in Figure 9 and Figure 10 in the Appendix. A comparison between the bed particle fusion data versus the microprobe analysis data (for some selected analytes) is presented in Table 4. A significant discrepancy was noted between the fusion and microprobe results for aluminum — 24.5 wt% versus 41.9 wt% respectively (see Appendix, Figure 10).

Triplicate fusion analysis for both the product and the fines was desired, and would provide better information regarding this potential compositional differences between the RSH-1 product and fines (as indicated by these initial fusion results); (it could also resolve the aluminum discrepancy between the fusion and microprobe results noted with the fines). Future work should address this issue.

RSH-1 250-300 um

	Particle 1, rim (wt.%)	Particle 1, core (wt.%)	Particle 2, rim (wt.%)	Particle 2, core (wt.%)
Na	1.23	0.4	1.29	0.54
Al	44.7	44.9	42	46.7
Ca	0.08	2.74	0.09	0.38
O	44.5	42.2	41.7	43
B	0.42	0.5	0.52	<0.2
N	1.34	0.71	1.61	0.56
F	<0.05	<0.05	<0.05	<0.05
C*	0.22	0.15	0.11	0.11

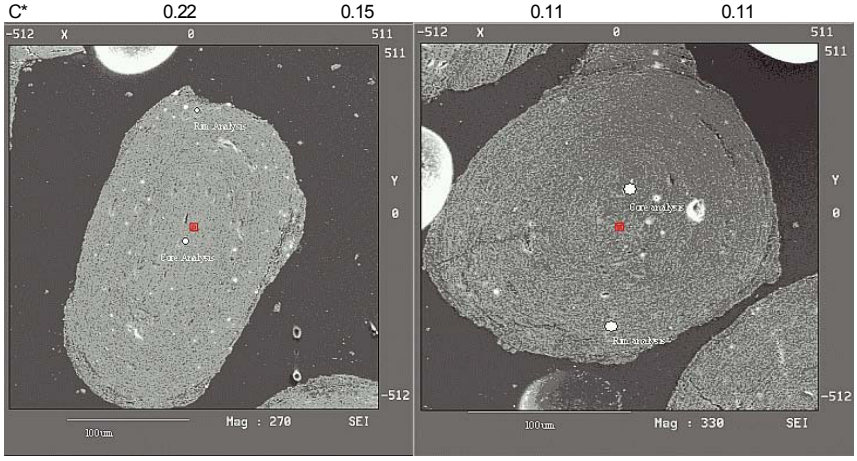

Figure 2. Electron microprobe analysis results; 250 to 300µm RSH-1 bed particles.

Table 4. Compare Bed Particle Fusion versus Microprobe Analyte Results Data.

Method	**Analyte**					
	Al	Na	Ca	B	O	C
Fusion wt%	45.54	1.94	0.35	0.32	-	-
Microprobe avg. wt %	44.1	0.92	0.50	0.52	42.48	0.12

Considering this limited data, the agreement between the bed particle fusion and microprobe results is reasonable. As alluded to earlier, triplicate fusion analysis and additional microprobe analyses were desired, but because of limited resources, were not requested. Triplicate analyses are recommended if better accuracy is necessary.

SEM photomicrographs were obtained for RSH-1 bed particle material (see Figure 3). A bed particle was fractured to obtain a view of a particle's interior; the highly porous and non-structured nature of the RSH-1 calcine was observed. A summary of RSH-1 bed material and fines XRD results is presented in Table 5.

Table 5. RSH-1 XRD Analysis Results

Sample Name	Results	Log#9902236
RSH-1 Product	This sample is mostly amorphous. Al_2O_3 (Corundum) and Al_2O_3 (gamma-Alumina) are present as minor components.	
RSH-1 Fines	$NaNO_3$ (nitratine) and also Al_2O_3 (Corundum) are the major crystalline components of this sample.	

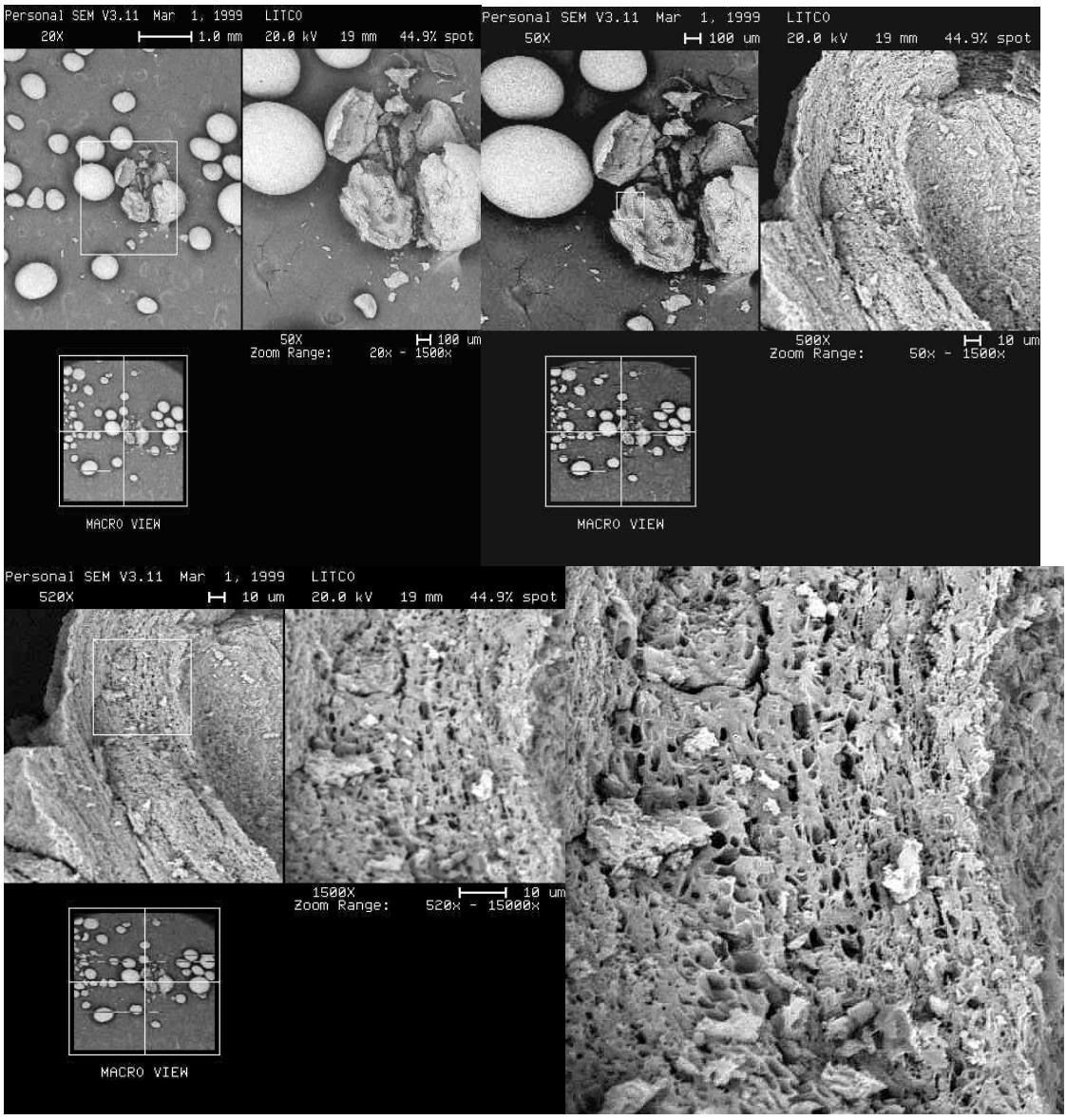

Figure 3. SEM photomicrographs of RSH-1 bed particles

4.1.1 Estimate RSH-1 Calcine Compounds

Similar to the work done by Brewer and Kessinger[6], a thermodynamic equilibrium program —HSC Chemistry® for Windows[7] —was utilized to estimate chemical compounds formed in RSH-1 during the calcination process. A species list was generated with this software from the elements in the RSH-1 flowsheet feed. Condensed solid phase species (calcine products) were also included in this species list. An equilibrium module input file was created from this list. The RSH-1 flowsheet aqueous feed composition component flowrates, the kerosene and O_2 flowrates, and the fluidizing air flowrate were entered into the input file (based on liters of feed per hour). By iteration with the Gibbs energy minimization equilibrium output results, the less thermodynamically stable solid compounds were pared from the input file; the gas and aqueous "IN" streams portion of this input file is presented in the Appendix, Table 11. The output results for the calcine compounds determined, at the bed mean temperature of 400°C, is presented in Table 6.

Table 6. Estimate of Calcine Compounds in RSH-1; HSC Equilibrium Calculations.

C:\RSH1R1.OGI

Components	Phase	Units	MW g/mol	Component mols @ 400^{0}C	Component mass(g/hr)	Component mass wt%
Al2O3(C)	3	kmol	101.961	6.13E-01	6.247E+01	36.926%
Al2O3	3	kmol	101.961	5.56E-01	5.668E+01	33.505%
Al2O3(K)	3	kmol	101.961	1.73E-01	1.767E+01	10.446%
Al2O3(D)	3	kmol	101.961	1.25E-01	1.270E+01	7.509%
NaNO3	3	kmol	84.995	1.09E-01	9.304E+00	5.500%
Al2O3(G)	3	kmol	101.961	2.87E-02	2.925E+00	1.729%
MgO*Al2O3	3	kmol	142.266	1.26E-02	1.789E+00	1.057%
CaCO3	3	kmol	100.089	1.18E-02	1.184E+00	0.700%
B2O3	3	kmol	69.618	1.19E-02	8.294E-01	0.490%
B2O3(G)	3	kmol	69.618	8.08E-03	5.626E-01	0.333%
CaCO3(A)	3	kmol	100.089	7.26E-03	7.267E-01	0.430%
CaO*2Al2O3	3	kmol	260.002	3.87E-03	1.006E+00	0.595%
NaCl	2	kmol	58.443	4.51E-03	2.636E-01	0.156%
Al2O3*H2O(B)	3	kmol	119.976	1.83E-03	2.190E-01	0.129%
Al2O3*SiO2(D)	3	kmol	162.046	1.74E-03	2.820E-01	0.167%
Fe2O3	3	kmol	159.692	1.25E-03	1.996E-01	0.118%
Al2O3*H2O	3	kmol	119.976	7.08E-04	8.497E-02	0.050%
HgO	3	kmol	216.589	6.21E-04	1.344E-01	0.079%
MgO	3	kmol	40.304	4.14E-04	1.668E-02	0.010%
MgO(M)	3	kmol	40.304	2.73E-04	1.102E-02	0.007%
Al2O3*SrO	3	kmol	205.581	2.10E-04	4.317E-02	0.026%
HgO(Y)	3	kmol	216.589	1.07E-04	2.309E-02	0.014%
Eu2O3	3	kmol	351.918	5.87E-05	2.065E-02	0.012%
CaO*Al2O3	3	kmol	158.041	3.53E-05	5.575E-03	0.003%
Eu2O3(M)	3	kmol	351.918	4.13E-05	1.455E-02	0.009%
MgO2	3	kmol	56.304	3.60E-05	2.027E-03	0.001%
MgCO3	3	kmol	84.314	2.04E-06	1.722E-04	0.000%
			Total calcine mass(g/hr) =		169.17	100.00%

Keep in mind these results are only an estimate. Calcination is not an equilibrium process and the rates of compound formation are unknown[8]. Although a mean bed temperature is

assumed, bed material undergoes a cyclic sequence of cooling and heating during its migration in the fluidized bed circulation pattern; where this cycle starts is arbitrary. Cooling occurs as material passes through the feed spray and is coated. Drying further cools the particle while some denitration/mineralization occurs. Drying, and then denitration/mineralization rates are accelerated when the material is heated due to the kerosene combustion; the material is ready for another cycle. This ideal cycle is the calcination period; the temperature amplitude during this period affects compound formation and crystal growth. Historically, XRD data has indicated that most of the calcine compounds are amorphous[6,9]. Transmission Electron Microscopy (TEM) technology is required to determine the scale of crystals in calcine.

The wt% of elements in this estimate of compounds in the RSH-1 was calculated; this result is presented in the Appendix, Table 12. The redundant compounds in Table 6 were combined (alumina most notably); this shorter compound list is presented in Table 13.

The element wt% results from this estimate made with HSC software are compared with the fusion and microprobe results in Table 7. These results were reasonably acceptable. The carbon result was interesting; the microprobe detected 0.12 wt% and the HSC estimated 0.14 wt% (due to 1.1 wt% $CaCO_3$ estimated in the RSH-1). Twenty-six wt% carbon was detected in a sample of fluorinel/sodium (Run17) pilot plant calcine via an X-Ray Physical Electron Spectroscopy method (XPS)[6]. Brewer and Kessinger concluded however that their result may have been due to surface contamination. The microprobe carbon results obtained here for RSH-1 are believed to be accurate. This carbon is part of calcine matrix, formed during the calcination process; it is not due to surface/atmospheric contamination[10]. Furthermore, it was concluded that the carbon is from the kerosene (as estimated by the HSC results).

Table 7. Compare HSC Estimated Element wt% Against Fusion/Microprobe Results.

Method	**Analyte**					
	Al	Na	Ca	B	O	C
Estimate from HSC Calcs	48.49	1.55	0.54	0.26	47.6	0.14
Fusion wt%	45.54	1.94	0.35	0.32	-	-
Microprob avg. wt %	44.1	0.92	0.50	0.52	42.48	0.12

Utilizing this HSC software estimate of compounds in the RSH-1, the mass conversion was back-calculated for the equilibrium/solubility inhibition liquid phase analytical data and compared with the actual mass conversion data (see § 4.2.5). This exercise was undertaken to validate using this technique for the kinetics testing with actual calcine at the INTEC Remote Analytical Laboratory (RAL). Performing these % mass dissolution kinetics tests remotely with actual calcine is virtually impossible — and would require significant amounts of calcine.

4.2 Baseline Dissolution Kinetics Testing Results

4.2.1 Calcine Consumption Coefficient Testing

The calcine acid consumption coefficient (**b**) was determined for RSH-1 bed product material. The test matrix results are presented in Table 8. An average value of **b** = 19.8 grams RSH-1 dissolved per mol of acid consumed was obtained.

Table 8. RSH-1 Calcine Acid Consumption Coefficient Testing Results.

Testing	Run Description	starting g calcine	g calcine dissolved	$Conversion_{mass}$	mol H^+ consumed	**b** g calcine dissolved / mol H^+ consumed
RSH-1 Bed Product	2g/100 ml of 4 M acid @ 60°C for 60 min.	1.8559	1.2663	0.682	7.00E-02	18.1
	2g/100 ml of 4 M acid @ >95°C for 60 min.	1.771	1.4058	0.794	6.16E-02	22.8
	2g/100 ml of 6 M acid @ >95°C for 60 min.	1.7949	1.4072	0.784	7.22E-02	19.5
	2g/100 ml of 6 M acid @ >95°C for 7 hrs.	1.7952	1.6456	0.917	8.71E-02	18.9

4.2.2 Order of Reaction Testing Results

The data from the *order of reaction* testing are presented in the Appendix, Table 14. The order of reaction was determined for the incipient rate of dissolution at time zero. To determine this, the mass dissolution data at the 1, 2, 3, 6, and 12 minute dissolution times was plotted versus time. This plot was curve-fit with a 3rd order non-uniform rational B-spline algorithm; this algorithm provides a smooth non-oscillating first derivative back to the origin. The first derivative of this function at time zero was the initial rate of dissolution — $dX/dt\big|_{@\ t\ =\ zero}$. Results for the 0.5 M data is presented in the Appendix, Figure 11. Curve-fitting results for this testing is presented in the Appendix, Table 15.

An initial dissolution rate was determined for each of the acid concentrations. If a plot of the ln{rate form} versus $\ln[H^+]$ yields a straight-line fit, then that rate form describes the initial dissolution rate, and the slope of the line is the order of reaction based on the acid concentration[11]. For the heterogeneous rate form — $\frac{m_0}{S_0}\frac{dX}{dt}\left[\frac{g\ dissolved}{cm^2\ \min}\right]$ was used, where S_0/m_0 is the initial surface area per gram of calcine. This was assumed a constant value over all the acid concentrations because the riffled same-size bed particle material was used throughout this testing. For the homogeneous rate form — $\frac{m_0}{V}\frac{dX}{dt}\left[\frac{g\ dissolved}{cm^3\ \min}\right]$ was used, where V is the dissolution volume at a given acid concentration. The ln{rate form} versus $\ln[H^+]$ for these two rate forms is shown in Figure 4.

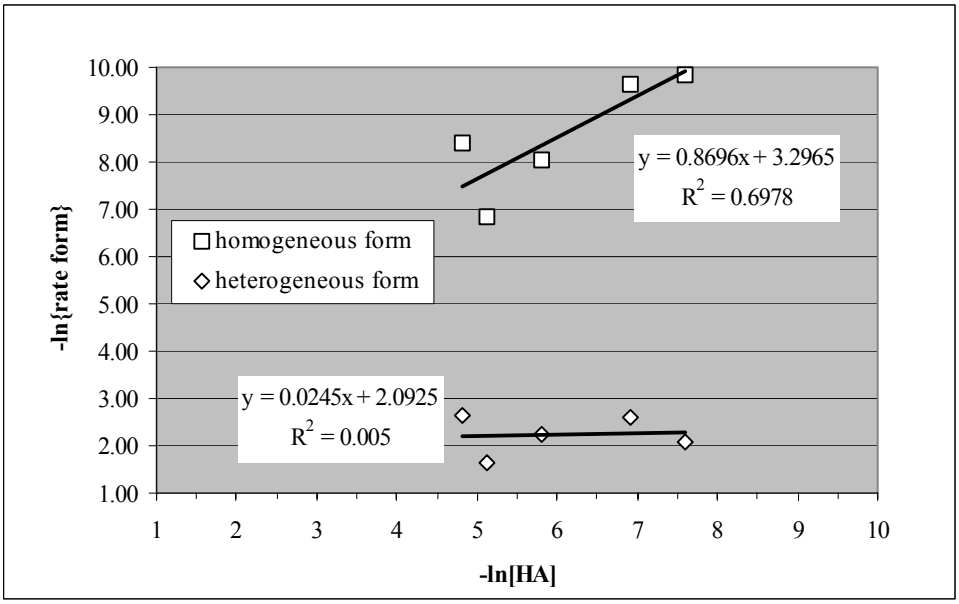

Figure 4. *Order of Reaction* Analysis; ln{rate form} versus ln $[H^+]$

These results were marginally satisfactory. As was observed for the Run74 zirconia pilot plant calcine testing, the homogeneous rate form fit the data better than the heterogeneous rate form[4]. The previous Run 74 testing was done with milled bed material, and that the testing done here with RSH-1 was with intact bed particles. These poor fit results were believed due to polydisperse dissolution — where the "parent" bed particle breaks apart into smaller particles as the dissolution progresses (as was observed for the Run74 testing).

An interesting result was observed when the RSH-1 alumina pilot plant calcine initial dissolution rate data was combined with the Run74 zirconia pilot plant calcine data to generate a plot of $\ln\{dX/dt|_{@0}\}$ versus $\ln\{\text{dia.}_0\}$. This combined data is presented in Table 9, and plotted in Figure 5.

Table 9. RSH-1 and Run 74 Combined Rate Data.

Material	d_0 (μm)	$\ln\{d_0\}$	dX/dt_0	$\ln\{dX/dt_0\}$
Milled Run74	58	4.06	0.384	-0.957
	69	4.23	0.333	-1.100
	90	4.50	0.274	-1.295
	116	4.75	0.252	-1.378
Milled RSH-1	137	4.92	0.223	-1.501
	275	5.62	0.176	-1.737
Run74 Bed Particle	462	6.14	0.198	-1.619
RSH-1 Bed Particle	475	6.16	0.192	-1.650
	655	6.48	0.108	-2.226
	925	6.83	0.0487	-3.022

From this plot, a characteristic *dissolution fractal dimension*, D_R, (as described in Ref. 12) was determined for milled pilot plant calcine material, and for bed particle material. A D_R of 2.51 was obtained for the milled calcine. Ulrich, et al[13] interpret $2.0 \leq D_R \leq 3.0$ to be in the regime of diffusion dissolution of non-Brownian particles. A D_R of 0.99 was obtained for the bed particle dissolution data; this was interpreted as dissolution of Smoluchowskian particles (particles for which the ratio of the particle radius to the electric double layer thickness is large[14]). It is pointed out that D_R, in addition to describing the dissolution process mechanism, "carries physically meaningful information about the growth process" (of the calcine bed particles). Continued review of dissolution phenomena in light of this fractal interpretation may provide some important and useful understanding of calcine structural characteristics, and of the calcine dissolution phenomena. The result from this fractal treatment of the dissolution data further supports the indication that calcine dissolution is more dependent upon its physical characteristics, rather than its chemical characteristics.

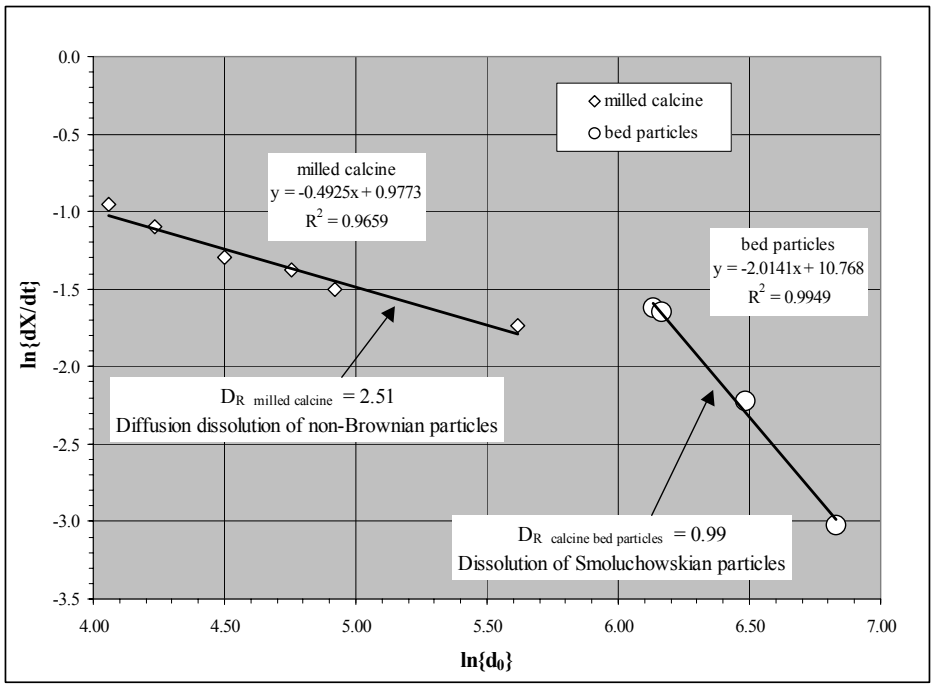

Figure 5. Fractal dimension interpretation of calcine dissolution.

4.2.3 Arrhenius Analysis Testing Results

Initial dissolution rates were determined from curvefit of the Arrhenius testing 1, 2, 3, 6, and 12 minute mass dissolution data at the respective temperatures. Mass conversion data and curvefit results are presented in Table 16 and Table 17. A plot of ln{rate} versus 1/T is presented in Figure 6. The slope of this line is E_A/R (see Ref. 11). From this plot, an *apparent activation energy* (E_A) of 26.9 kcal/mol was determined for RSH-1 alumina pilot plant calcine under conditions of 6 M unchanging acid concentration. This result was satisfactorily in line with typical values of 10-to-30 kcal/mol for mineral dissolution[15].

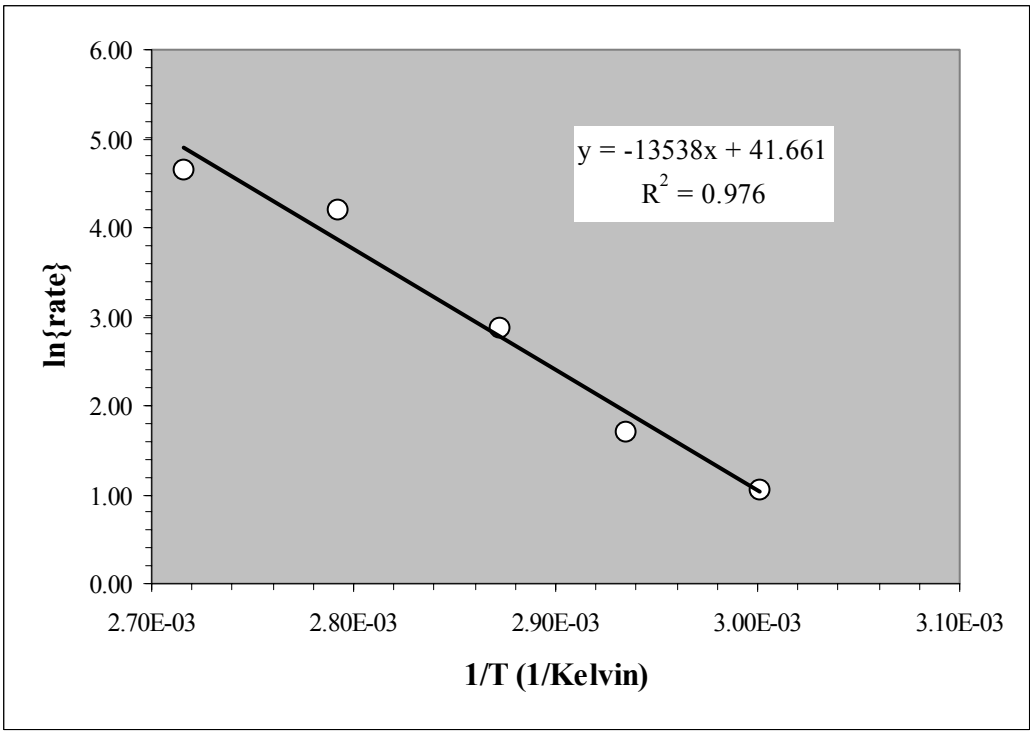

Figure 6. Arrhenius analysis plot

4.2.4 Dissolution Rate Controlling Mechanism Testing Results

The *dissolution rate controlling* determination testing was completed. The dissolution data results for this testing is presented in the Appendix, Table 18. These data were curvefit to determine the time required to achieve a given mass conversion. At the given mass conversion, the time and the corresponding particle size were paired; these results are presented in the Appendix, Table 19. A plot of $\ln\{time|_{@x}\}$ versus $\ln\{\text{dia.}_0\}$ was generated to determine the dissolution rate controlling mechanism. If the slope is unity, dissolution is reaction rate controlled; if the slope is 1.5 to 2—dissolution is film mass transfer controlled; and if the slope is 2, then dissolution is internal diffusion controlled[11]. This plot is shown in Figure 7.

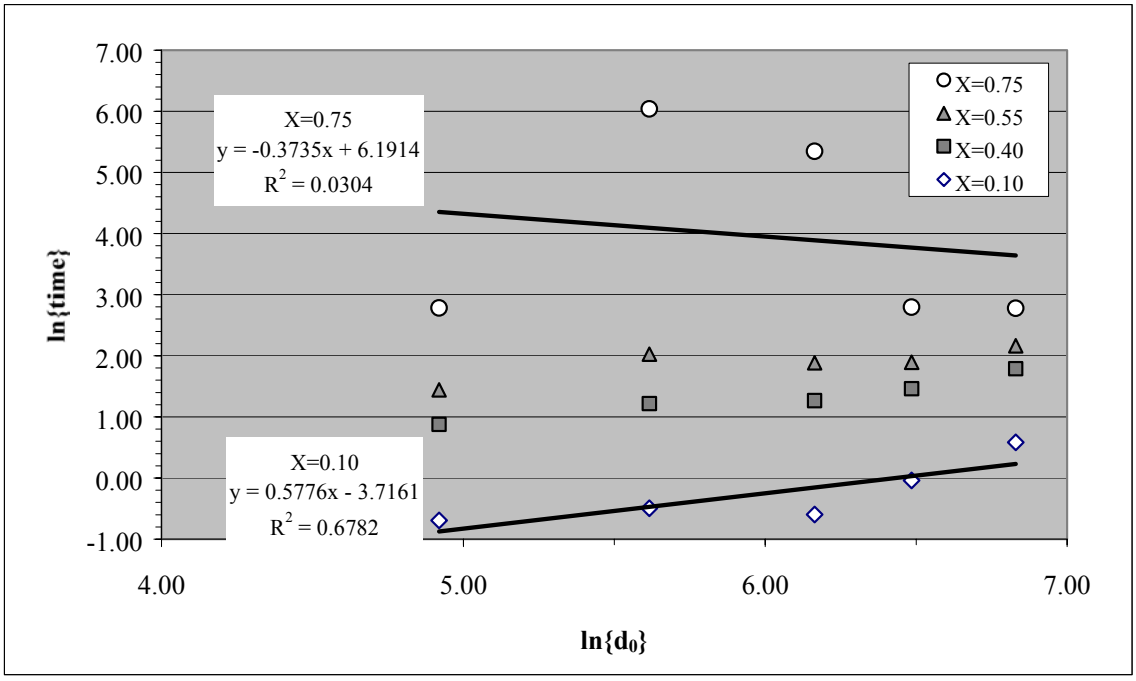

Figure 7. Rate controlling determination; ln{time} vs. ln{d_0}.

These results are marginal. The scatter in the data, especially at the higher conversion, was believed to be a result of dissolution in a polydisperse regime (as noted in the order of reaction results section). In the kinetics work done with the Run74 zirconia pilot plant calcine, rate controlling testing was performed exclusively with milled bed material; a more satisfactory fit was observed for that data. Nevertheless, it was noted that, just as with all previous calcine dissolution testing, this testing with RSH-1 showed the familiar initial rapid dissolution then the leveling-out of the rate, and the non-attainment of 100% dissolution after long dissolution times—indicating the characteristics of internal mass diffusion controlled dissolution.

4.2.5 Equilibrium/Solubility Inhibition Testing Results

The liquid phase analytical analyses results for the 1, 2, 3, 6, and 12 minute Arrhenius testing were combined with analyses results from the 1 and 6 hour tests (75ºC data). These analytical analysis results are presented in the Appendix, Table 20. Component conversion was calculated based on the liquid phase concentration data and the fusion analyses results; these results are presented in Table 21 and Table 22. The plot of component conversion versus time is presented in Figure 8. If component liquid phase concentrations increased at first, but then decreased at longer times, then solubility inhibition of complete dissolution is indicated. This was not the case observed for these RSH-1 testing results (see Figure 8). It was concluded that, because aluminum comprised the majority of the calcine wt%, the slowing dissolution rate of alumina compounds was preventing complete dissolution — the data does not suggest that complete dissolution of RSH-1 calcine is equilibrium/solubility inhibited.

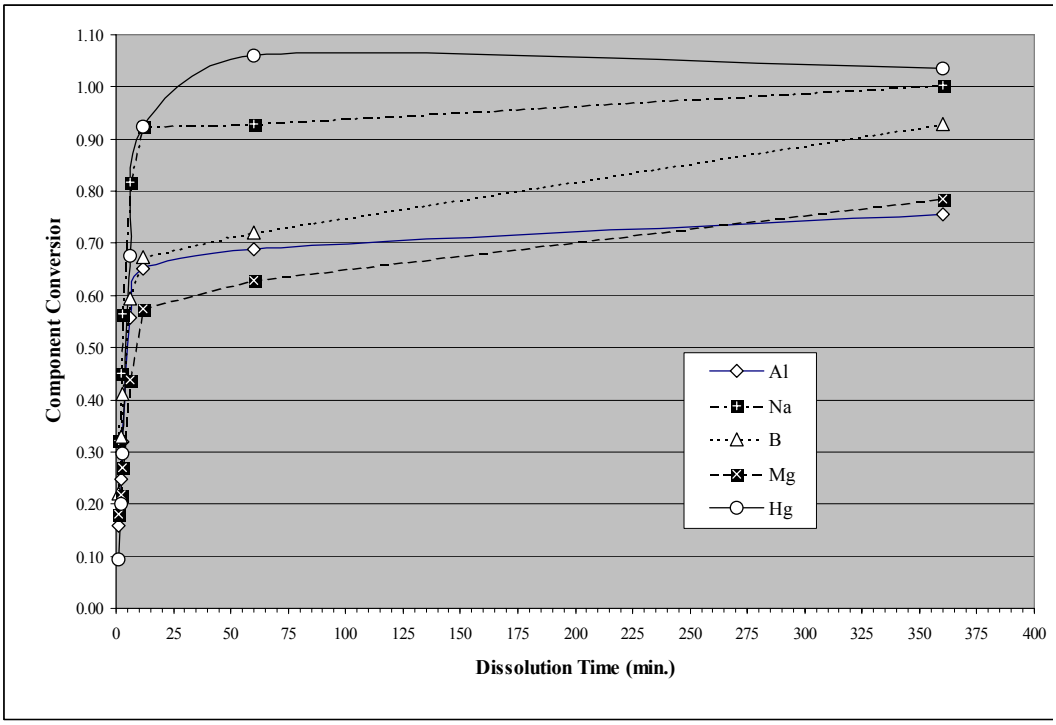

Figure 8. RSH-1 Component Conversion vs. Time; 6 M 75ºC data.

Mass conversion was back-calculated from these liquid phase component conversion results and the HSC software estimated wt% of compounds in the RSH-1 (the combined compound wt%'s were used; Table 12). These results are compared with the experimentally obtained mass conversions in Table 10. Overall, this technique is reasonably accurate for estimating % mass dissolution from liquid phase analytical chemistry data. It is recommended estimating mass conversion for dissolution testing with actual calcine at the RAL. The greatest relative difference was noted for times less than 5 minutes into the dissolution. This caused a 10% error in the evaluation of $dX/dt\Big|_{@\ t\ =\ zero}$; the value from the experimental mass dissolution data was 0.192 versus a value of 0.172 derived for the HSC estimated % mass dissolution.

Table 10. Comparison of Mass Conversion; Experimental vs. Back-Calculated.

Time (min)	Exp X	Calc X	% diff
1	0.192	0.172	11.1%
2	0.279	0.263	5.9%
3	0.38	0.338	11.2%
6	0.552	0.575	-4.1%
12	0.683	0.673	1.5%
60	0.713	0.707	0.8%
360	0.789	0.779	1.2%

The greatest percent mass dissolution observed during this testing with RSH-1 was 93.0 % (see Table 16). This was achieved after eight hours of dissolution at 95ºC.

5. CONCLUSIONS AND RECOMMENDATIONS

The conclusions and recommendations based on the results of this work follow:

1. Chemical and physical analyses were performed on the RSH-1 alumina type pilot plant calcine bed material. Elemental fusion analysis results agree well with microprobe analysis results. Results of thermodynamic modeling to estimate the chemical compounds in RSH-1 were reasonably acceptable when compared with the fusion and microprobe results. Triplicate fusion analysis and additional microprobe analyses, although these are resource taxing, are recommended if better accuracy is necessary.

2. Baseline dissolution kinetics testing was completed:

   - The calcine acid consumption coefficient was determined for RSH-1 bed product material. An average value of **b** = 19.8 grams RSH-1 dissolved per mol of acid consumed was obtained.

   - *Order of reaction* testing indicated that the homogeneous rate form fit the rate data better than the heterogeneous rate form. This was also observed for previous dissolution kinetics work done with zirconia-type pilot plant calcine. A characteristic *dissolution fractal dimension*, D_R, was determined for alumina and zirconia pilot plant calcine milled material and bed particles. The result from this fractal treatment of the dissolution data further supports the indication that calcine dissolution is more dependent upon its physical characteristics, rather than its chemical characteristics.

   - Arrhenius testing yielded an *apparent activation energy* (E_A) of 26.9 kcal/mol for RSH-1 alumina pilot plant calcine under conditions of constant 6 M acid concentration. This result is comparable to typical values for mineral dissolution.

   - The results from the *dissolution rate controlling* mechanism tests were inconclusive; data scatter was attributed to polydisperse dissolution of the bed particles. Nevertheless, as was observed in the previous zirconia pilot plant calcine dissolution kinetics work, there was the familiar initial rapid dissolution, then the leveling-out of the rate, and the non-attainment of 100% dissolution after long dissolution times. The RSH-1 dissolution kinetics also had the characteristics of internal mass diffusion controlled dissolution.

   - The equilibrium/solubility inhibition testing results indicated that the slowing dissolution rate of alumina compounds was preventing complete dissolution. The data does not suggest that complete dissolution of RSH-1 calcine is equilibrium/solubility inhibited. The greatest percent mass dissolution observed during this testing with RSH-1 was 93.0 %; this was achieved after eight hours of dissolution at 95ºC.

3. In conjunction with the compound estimates from the thermodynamic modeling, mass conversion was back-calculated from liquid phase compound conversion results. This technique is reasonably accurate for estimating the mass conversion from liquid phase analytical chemistry data. This exercise was undertaken to validate using this technique for the kinetics testing with actual calcine at the INTEC Remote Analytical Laboratory. Performing these % mass dissolution kinetics tests remotely with actual calcine is virtually impossible — and would require a significant amount of radioactive calcine. Utilization of this technique is recommended for estimating mass conversion for kinetics testing with actual calcine in the future. Triplicate fusion analysis on actual calcine to be used in kinetics testing is recommended.

6. REFERENCES

1. U. S. Department of Energy, "Idaho High-Level Waste and Facilities Disposition Draft Environmental; Impact Statement", DOE/EIS-0287D, December 1999.

2. B. J. Newby, "Dissolution and Disintegration of Calcine Clinkers", EINCO Internal Letter Report NBY-15-79 to K. F. Childs, November 1979.

3. K. N. Brewer, "Dissolution Scoping Tests on Two and Three-Way Blend Calcine", WINCO Internal Letter Report KNB-2-91 to B. H. O'Brien, March 19991.

4. T. A. Batcheller, "Dissolution Kinetics of Zirconia Calcine", INEEL/EXT-99-00566, June 1999.

5. R. S. Herbst, Idaho National Engineering and Environmental Laboratory, personal communication.

6. K. N. Brewer, G. F. Kessinger, L. L. Littleton, A. L. Olson, "Physical and Chemical Characteristics of Fluorinel/Sodium Calcine Generated during 30cm Pilot-plant Run17", WINCO-1139, July 1993.

7. Roine, Outokumpu HSC Chemistry® for Windows, Chemical Reaction and Equilibrium Software with Extensive Thermochemical Database, Version 4.1, Outokumpu Research Oy Information Service, PO Box 60, FIN-28101 Pori, Finland; available from ESM Software, 2235 Wade Court, Hamilton, Ohio 45013.

8. B. H. O'Brien, "Estimation of Alkali Metal Mole Percent and Weight of Calcined Solids for ICPP Calcine", INEL-95/0184, March 1995.

9. J. R. Berreth, "Inventories and Properties of ICPP Calcined High-Level Waste", WINCO-1050, February 1988.

10. K. E. Wright, Idaho National Engineering and Environmental Laboratory, personal communication.

11. O. Levenspiel, *Chemical Reaction Engineering*, John Wiley & Sons, 1972.

12. D. Avnir, *Fractal Approach to Heterogeneous Chemistry*, John Wiley & Sons Ltd., 1992.

13. M. Momonaga, J. Stavek, J. Ulrich, "Interpretation of Dissolution Rates by the Reaction Fractal Dimension", *Journal of Crystal Growth*, **166**, 1053 (1996).

14. D. J. Shaw, *Introduction to Colloid and Surface Chemistry*, Butterworth & Co. Ltd., 1980.

15. F. Habashi, *Principals of Extractive Metallurgy*, Gordon and Breach, New York, 1969.

APPENDIX

Test Results Data

Microprobe Analyses of RSH-1 Calcine

RSH-1, 32 mesh

	Particle 1, rim (wt.%	article 1, core (wt.%	article 2, rim (wt.%	Particle 2, core (wt.%)
Na	1.08	0.45	1.26	1.09
Al	42.7	44.4	44	43.6
Ca	0.09	0.41	0.09	0.1
O	42.7	40.3	45	43.9
B	0.46	<0.2	0.36	0.33
N	1.22	<0.5	1.82	1.47
F	<0.05	<0.05	<0.05	<0.05
C*	0.09	0.05	not measured	not measured

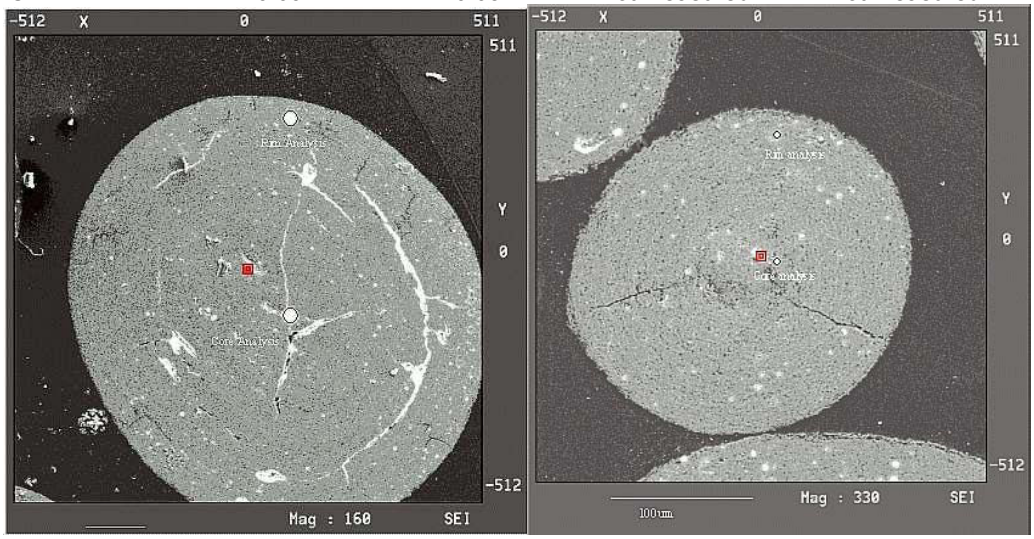

Figure 9. Electron microprobe results for 475µm RSH-1 bed particles.

Microprobe Analyses of RSH-1 Calcine

RSH-1 fines

	Particle 1, rim (wt.%	article 1, core (wt.%	article 2, rim (wt.%	Particle 2, core (wt.%)
Na	1.11	1.12	1.51	1.91
Al	41.2	43.3	41	42.1
Ca	0.04	0.07	0.06	0.15
O	41.5	43.7	41.4	41.3
B	<0.2	0.22	0.44	0.38
N	1.77	1.42	1.58	1.31
F	<0.05	<0.05	<0.05	<0.05
C*	1.67	0.64	not measured	not measured

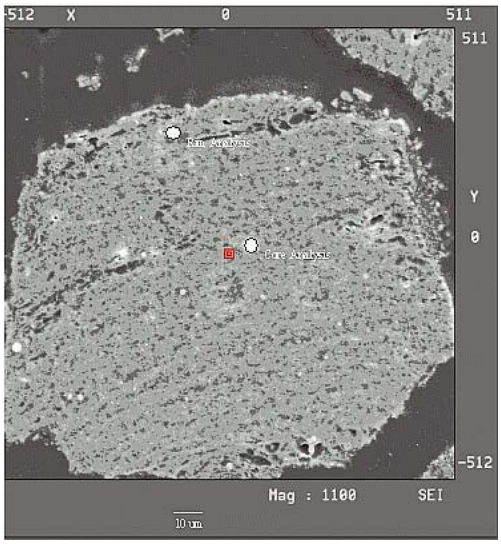

Figure 10. Microprobe analysis of RSH-1 fines particle

HSC Chemistry Input File for RSH-1 Calcine

Table 11. HSC Input File

	A	B	C	D
1	SPECIES Formula	Temp ^{0}C	mols/hr	mol %
2	**Gases**		217.680	100.000
3	CO(g)	25.000		
4	CO2(g)	25.000		
5	Cl2(g)	25.000		
6	H2O(g)	25.000		
7	Hg(g)	25.000		
8	HgCl2(g)	25.000		
9	N2(g)	25.000	127.400	58.526
10	NO(g)	25.000		
11	NO3(g)	25.000		
12	NO2(g)	25.000		
13	O2(g)	25.000	87.900	40.380
14	C12H26(DODg)	25.000	2.380	1.093
15	**Aqueous**		116.054	100.000
16	H2O	25.000	100.000	86.167
17	Al(+3a)	25.000	3.040	2.619
18	Al(NO3)3(a)	25.000		
19	BH4(-a)	25.000		
20	BO2(-a)	25.000	0.040	0.034
21	CO2(a)	25.000		
22	Ca(+2a)	25.000	0.023	0.020
23	CaCO3(a)	25.000		
24	Cl2(a)	25.000		
25	Cl(-a)	25.000	0.005	0.004
26	Cs(+a)	25.000	0.000	0.000
27	CsCl(a)	25.000		
28	Eu(+4a)	25.000		
29	Eu(+3a)	25.000	0.000	0.000
30	Eu(+2a)	25.000		
31	Fe(+3a)	25.000	0.003	0.002
32	Fe(+2a)	25.000		
33	H(+a)	25.000	1.588	1.368
34	HNO2(a)	25.000		
35	HNO3(a)	25.000		
36	Hg(a)	25.000		
37	Hg(+2a)	25.000	0.024	0.021
38	Mg(+2a)	25.000	0.013	0.011
39	N2(a)	25.000		
40	NO2(-a)	25.000		
41	NO3(-a)	25.000	11.054	9.525
42	NH4(+a)	25.000	0.148	0.127
43	Na(+a)	25.000	0.114	0.098
44	NaCO3(-a)	25.000		
45	O2(a)	25.000		
46	O(-a)	25.000		
47	O2(-a)	25.000		
48	O2(-2a)	25.000		

HSC Chemistry Wt% Elements in RSH-1 Calcine

Table 12. HSC Wt% Elements in RSH-1

Components	Al	Na	Mg	Ca	C	B	Si	Fe	Hg	Sr	Eu	N	Cl	Oxygen	
Al2O3(C)	19.54%													17.38%	
Al2O3	17.73%													15.77%	
Al2O3(K)	5.53%													4.92%	
Al2O3(D)	3.97%													3.53%	
NaNO3		1.49%										0.91%		3.11%	
Al2O3(G)	0.92%													0.81%	
MgO*Al2O3	0.40%		0.18%											0.48%	
CaCO3				0.28%	0.08%									0.34%	
B2O3						0.15%								0.34%	
B2O3(G)						0.10%								0.23%	
CaCO3(A)				0.17%	0.05%									0.21%	
CaO*2Al2O3	0.25%			0.09%										0.26%	
NaCl		0.06%											0.09%		
Al2O3*H2O(B)	0.06%													0.07%	
Al2O3*SiO2(D)	0.06%						0.03%							0.08%	
Fe2O3								0.08%						0.04%	
Al2O3*H2O	0.02%													0.03%	
HgO									0.07%					0.01%	
MgO			0.01%											0.00%	
MgO(M)			0.00%											0.00%	
Al2O3*SrO	0.01%									0.01%				0.01%	
HgO(Y)									0.01%					0.00%	
Eu2O3											0.01%				
CaO*Al2O3	0.00%			0.00%											
Eu2O3(M)											0.01%				
MgO2															
MgCO3															
Totals	48.49%	1.55%	0.19%	0.54%	0.14%	0.26%	0.03%	0.08%	0.09%	0.01%	0.02%	0.91%	0.09%	47.60%	99.99%
	Al	**Na**	**Mg**	**Ca**	**C**	**B**	**Si**	**Fe**	**Hg**	**Sr**	**Eu**	**N**	**Cl**	**Oxygen**	**Total**

HSC Chemistry Primary Compounds in RSH-1 Calcine

Table 13. HSC Primary Compounds in RSH-1

Components	Al2O3	NaNO3	MgO	CaCO3	B2O3	CaO	NaCl	H2O	SiO2	Fe2O3	HgO	SrO	Eu2O3	MgO2	
Al2O3(C)	36.93%														
Al2O3	33.51%														
Al2O3(K)	10.45%														
Al2O3(D)	7.51%														
NaNO3		5.50%													
Al2O3(G)	1.73%														
MgO*Al2O3	0.76%		0.30%												
CaCO3				0.70%											
B2O3					0.49%										
B2O3(G)					0.33%										
CaCO3(A)				0.43%											
CaO*2Al2O3	0.47%					0.13%									
NaCl							0.16%								
Al2O3*H2O(B)	0.11%							0.02%							
Al2O3*SiO2(D)	0.10%								0.06%						
Fe2O3										0.12%					
Al2O3*H2O	0.04%							0.01%							
HgO											0.08%				
MgO			0.01%												
MgO(M)			0.01%												
Al2O3*SrO	0.01%											0.01%			
HgO(Y)											0.01%				
Eu2O3													0.01%		
CaO*Al2O3	0.00%					0.00%									
Eu2O3(M)													0.01%		
MgO2														0.00%	
Totals	91.61%	5.50%	0.32%	1.13%	0.82%	0.13%	0.16%	0.03%	0.06%	0.12%	0.09%	0.01%	0.02%	0.00%	100.00%
	Al2O3	NaNO3	MgO	CaCO3	B2O3	CaO	NaCl	H2O	SiO2	Fe2O3	HgO	SrO	Eu2O3	MgO2	Total

Order of Reaction Testing Data

Table 14. *Order of Reaction* Testing Data.

0.5 Molar Data

time (min)	X @ t	mass calcine (g)	filter @ 0 (g)	filter @ t (g)
0	0	-	-	-
1	0.126	0.4616	73.1518	73.5553
2	0.213	0.3865	71.9304	72.2347
3	0.259	0.4646	73.0726	73.4168
6	0.423	0.3881	72.4535	72.6775
12	0.661	0.3762	73.5171	73.6446

1 Molar Data

0	0	-	-	-
1	0.073	0.4445	73.0183	73.4305
2	0.134	0.4713	72.7395	73.1476
3	0.210	0.4345	72.7614	73.1045
6	0.409	0.4434	72.6325	72.8945
12	0.633	0.4472	72.8575	73.0216

3 Molar Data

0	0	-	-	-
1	0.107	1.1921	73.2254	74.2897
2	0.187	1.1961	72.7234	73.6957
3	0.280	1.1141	73.4635	74.2651
6	0.510	1.2771	73.3800	74.0053
12	0.682	1.2240	71.9127	72.3024

6 Molar Data

0	0	-	-	-
1	0.193	2.1816	72.5125	74.2738
2	0.279	2.2092	72.1593	73.7516
3	0.375	2.1560	72.3538	73.7020
6	0.539	2.1742	72.3054	73.3078
12	0.694	2.2373	72.385	73.0691
60	0.713	2.2437	71.9823	72.6269
360	0.789	1.0133	72.0362	72.2500

8 Molar Data

0	0	-	-	-
1	0.072	1.2230	73.0020	74.1373
2	0.143	1.2410	72.8082	73.8719
3	0.232	1.2558	73.2086	74.1734
6	0.431	1.2035	72.6353	73.3195
12	0.638	1.2897	71.9868	72.4541

Determine $dX/dt\Big|_{@\ t\ =\ zero}$ for *Order of Reaction* Testing

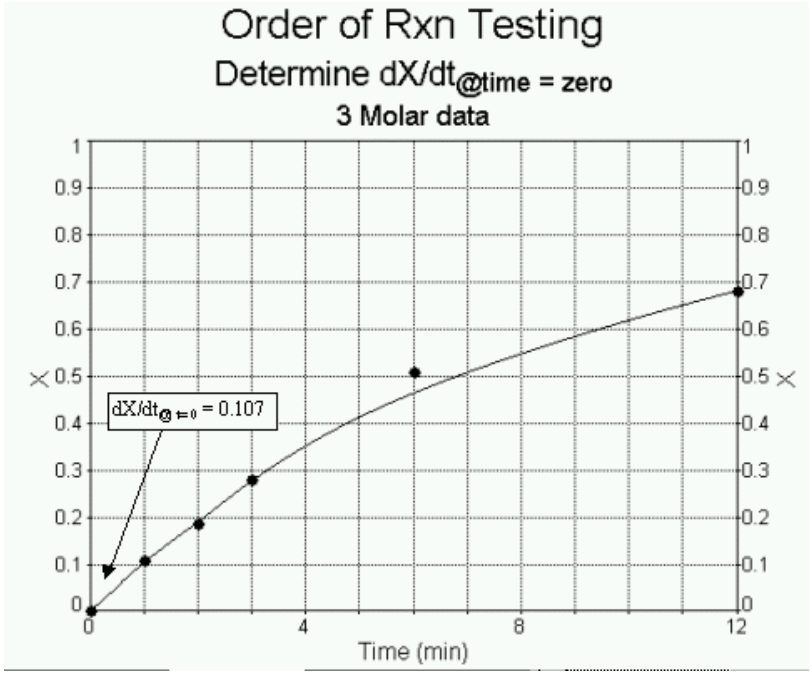

Figure 11. 3rd order non-uniform rational B-spline curvefit of 3 M *Order of Reaction* test data.

Table 15. Order of Reaction Initial Rate Curve Fit Results and Rate Forms.

Molar	[acid] (mol/ml)	-ln{acid}	dX/dt	-ln{dX/dt}	m_0 (gram)	Vol (mls)	{homog form}	-ln{homog form}
0.5	0.0005	7.60	0.126	2.07	0.4154	1000	5.23E-05	9.86
1	0.001	6.91	0.073	2.62	0.4481	500	6.54E-05	9.63
3	0.003	5.81	0.107	2.23	1.2007	400	3.21E-04	8.04
6	0.006	5.12	0.192	1.65	2.1916	400	1.05E-03	6.86
8	0.008	4.83	0.072	2.63	1.2426	400	2.24E-04	8.41

Arrhenius Testing Data Results

Table 16. Arrhenius Testing Data Results

% Mass Conversion	Time (min)							
Temperature (^{0}C)	1	2	3	6	12	60	360	480
60.0	2.3	3.3	6.5	17.5	33.0	-	-	-
67.5	3.8	10.1	14.7	31.5	-	-	-	-
75.0	18.0	27.2	37.6	54.6	69.0	71.3	78.9	
85.0	44.4	60.3	64.6	70.5	72.8	-	-	-
95.0	55.3	66.0	69.4	70.6	72.3	78.9	-	93.0

Table 17. Arrhenius Testing Data Curve-fit Results.

T ^{0}C	1/T	Rate (curve-fit)	ln{Rate}
95.0	2.72E-03	104.70	4.651
85.0	2.79E-03	67.10	4.206
75.0	2.87E-03	17.60	2.868
67.5	2.94E-03	5.50	1.705
60.0	3.00E-03	2.88	1.058

Dissolution Rate Controlling Mechanism Testing Data

Table 18. Dissolution Rate Controlling Testing Data.

125 to 150µm data

time (min)	X @ t	mass calcine (g)	filter @ 0 (g)	filter @ t (g)
0	0	-	-	-
2	0.447	2.1608	72.8585	74.0530
6	0.644	2.0915	72.8426	73.5873
12	0.752	2.2160	73.0045	73.5548
30	0.780	2.2090	73.4074	73.8938
60	0.798	2.1889	72.6953	73.1383
420	0.857	2.2135	72.6834	72.9998

250 to 300µm data

0	0	-	-	-
2	0.353	2.2457	72.1896	73.6432
6	0.536	2.2184	73.1596	74.1892
12	0.609	2.2013	73.345	74.2054
30	0.638	2.1658	72.3573	73.1413
60	0.649	2.1740	72.9271	73.6909
420	0.747	2.2218	73.3942	73.9569

355 to 595µm data

0	0	-	-	-
1	0.193	2.1816	72.5125	74.2738
2	0.279	2.2092	72.1593	73.7516
3	0.375	2.1560	72.3538	73.7020
6	0.539	2.1742	72.3054	73.3078
12	0.694	2.2373	72.385	73.0691
60	0.713	2.2437	71.9823	72.6269
360	0.789	1.0133	72.0362	72.2500

600 to 710µm data

0	0	-	-	-
2	0.216	2.1138	72.9622	74.6195
6	0.549	2.2418	72.0167	73.0285
12	0.744	2.2694	73.2036	73.7835
30	0.822	2.2985	73.3774	73.7875
60	0.830	2.1368	72.293	72.6570
420	0.873	2.1367	72.7645	73.0351

850 to 1000µm data

0	0	-	-	-
2	0.097	2.2753	73.2819	75.3359
6	0.421	2.2158	73.1315	74.4140
12	0.730	2.1438	71.9145	72.4930
30	0.909	2.1744	73.3122	73.5109
60	0.915	2.2211	73.2449	73.4340
420	0.935	2.1946	71.6587	71.8023

Dissolution Rate Controlling Mechanism Testing Data Curve-fit Results

Table 19. Dissolution Rate Controlling Mechanism Data Curve-fit Results.

dnot (μm)	time @ X	ln{dnot}	ln{time}
	X=0.10		
137	0.50	4.92	-0.69
275	0.61	5.62	-0.49
475	0.55	6.16	-0.60
655	0.96	6.48	-0.04
925	1.79	6.83	0.58
	X=0.40		
137	2.40	4.92	0.88
275	3.37	5.62	1.21
475	3.54	6.16	1.26
655	4.31	6.48	1.46
925	5.98	6.83	1.79
	X=0.55		
137	4.23	4.92	1.44
275	7.58	5.62	2.03
475	6.59	6.16	1.89
655	6.65	6.48	1.89
925	8.72	6.83	2.17
	X=0.75		
137	16.20	4.92	2.79
275	420.00	5.62	6.04
475	210.00	6.16	5.35
655	16.36	6.48	2.79
925	16.12	6.83	2.78

Equilibrium/Solubility Inhibition Testing Liquid Phase Analytical Results

Table 20. Equilibrium/Solubility Inhibition Testing Liquid Phase Analytical Results.

RSH Arrhenius plot "component conversion vs time"

Experimental parameters: 2gm/400 mls, 6 M nitric acid, 75 C

	(log # 010320-2)	Elemental data (µg/mL)					
	1 Min	2 Min	3 Min	6 Min	12 Min	60 min	6 hrs
Aluminum	393.357	621.291	788.366	1418.5	1601.5	1.76E+03	1.74E+03
Boron	3.8159	5.7783	7.0807	10.5501	11.539	1.29E+01	1.49E+01
Calcium	7.4921	9.9209	12.672	16.236	19.382	2.04E+01	2.33E+01
Cesium	2.16E-01	3.30E-01	4.04E-01	6.29E-01	6.94E-01	7.17E-01	6.46E-01
Chloride	7.4	7.4	7.4	6.08E+02	3.77E+01	0.3715	0.3715
Europium	0.3135	0.4851	0.6193	0.9933	1.1088	1.17E+00	1.11E+00
Iron	1.0604	0.9713	0.9867	0.9944	2.1736	1.23E+00	1.70E+00
Magnesium	1.9635	2.3936	2.9216	4.8851	6.1644	7.03E+00	7.92E+00
Mercury	2.29	4.95	7.19	16.9	22.2	26.5	23.4
Silicon	0.1804	0.2123	0.3256	0.3498	0.5951	5.49E-01	1.91E+00
Sodium	3.42E+01	4.83E+01	5.96E+01	8.86E+01	9.66E+01	1.01E+02	9.86E+01

Equilibrium/Solubility Inhibition Testing Elemental Conversion Results

Table 21. Equilibrium/Solubility Inhibition Testing Elemental Conversion Results.

Data from 1st set of dissolutions

	Starting Mass(gms)	Volume (mLs)	$Al_{Initial}$	Al_{Final}	Conversion ($Al_{Final}/Al_{Initial}$)	Time (minutes)
Aluminum	2.1816	400	0.9936	0.1573	0.1584	1
	2.2092	400	1.0062	0.2485	0.2470	2
	2.1742	400	0.9902	0.3153	0.3185	3
	2.2373	400	1.0190	0.5674	0.5568	6
	2.1560	400	0.9820	0.6406	0.6524	12
	2.2437	400	1.0219	0.7044	0.6893	60
	1.0133	200	0.4615	0.3489	0.7560	360

	Starting Mass(gms)	Volume (mLs)	$B_{Initial}$	B_{final}	Conversion ($B_{Final}/B_{Initial}$)	Time (minutes)
Boron	2.1816	400	0.0069	0.0015	0.2204	1
	2.2092	400	0.0070	0.0023	0.3296	2
	2.1742	400	0.0069	0.0028	0.4104	3
	2.2373	400	0.0071	0.0042	0.5942	6
	2.1560	400	0.0068	0.0046	0.6744	12
	2.2437	400	0.0071	0.0051	0.7222	60
	1.0133	200	0.0032	0.0030	0.9294	360

	Starting Mass(gms)	Volume (mLs)	$Ca_{Initial}$	Ca_{Final}(avg.)	Conversion ($Ca_{Final}/Ca_{Initial}$)	Time (minutes)
Calcium	2.1816	400	0.0076	0.0030	0.3967	1
	2.2092	400	0.0076	0.0040	0.5188	2
	2.1742	400	0.0075	0.0051	0.6733	3
	2.2373	400	0.0077	0.0065	0.8383	6
	2.1560	400	0.0075	0.0078	1.0385	12
	2.2437	400	0.0078	0.0082	1.0511	60
	1.0133	200	0.0035	0.0047	1.3273	360

	Starting Mass(gms)	Volume (mLs)	$Cs_{Initial}$	Cs_{Final}	Conversion ($Cs_{Final}/Cs_{Initial}$)	Time (minutes)
Cesium	2.1816	400	0.0004	0.0001	0.2371	1
	2.2092	400	0.0004	0.0001	0.3578	2
	2.1742	400	0.0004	0.0002	0.4451	3
	2.2373	400	0.0004	0.0003	0.6734	6
	2.1560	400	0.0004	0.0003	0.7710	12
	2.2437	400	0.0004	0.0003	0.7654	60
	1.0133	200	0.0002	0.0001	0.7635	360

	Starting Mass(gms)	Volume (mLs)	$Cl_{Initial}$	Cl_{Final}	Conversion ($Cl_{Final}/Cl_{Initial}$)	Time (minutes)
Chloride	2.1816	400	0.0954	0.0030	0.0310	1
	2.2092	400	0.0966	0.0030	0.0307	2
	2.1742	400	0.0950	0.0030	0.0311	3
	2.2373	400	0.0978	0.2432	2.4868	6
	2.1560	400	0.0942	0.0151	0.1600	12
	2.2437	400	0.0981	0.0001	0.0015	60
	1.0133	200	0.0443	0.0001	0.0017	360

Equilibrium/Solubility Inhibition Testing Component Conversion Results (cont.)

Table 22. Equilibrium/Solubility Inhibition Testing Elemental Conversion Results (cont.).

	Starting Mass(gms)	Volume (mLs)	$Eu_{Initial}$	Eu_{Final}	Conversion ($Eu_{Final}/Eu_{Initial}$)	Time (minutes)
Europium	2.1816	400	0.0006	0.0001	0.2183	1
	2.2092	400	0.0006	0.0002	0.3336	2
	2.1742	400	0.0006	0.0002	0.4327	3
	2.2373	400	0.0006	0.0004	0.6745	6
	2.1560	400	0.0006	0.0004	0.7813	12
	2.2437	400	0.0006	0.0005	0.7925	60
	1.0133	200	0.0003	0.0002	0.8320	360
	Starting Mass(gms)	Volume (mLs)	$Fe_{Initial}$	Fe_{Final}(avg.)	Conversion ($Fe_{Final}/Fe_{Initial}$)	Time (minutes)
Iron	2.1816	400	0.0008	0.0004	0.5208	1
	2.2092	400	0.0008	0.0004	0.4711	2
	2.1742	400	0.0008	0.0004	0.4863	3
	2.2373	400	0.0008	0.0004	0.4762	6
	2.1560	400	0.0008	0.0009	1.0802	12
	2.2437	400	0.0008	0.0005	0.5889	60
	1.0133	200	0.0004	0.0003	0.8979	360
	Starting Mass(gms)	Volume (mLs)	$Mg_{Initial}$	Mg_{Final}(avg.)	Conversion ($Mg_{Final}/Mg_{Initial}$)	Time (minutes)
Magnesium	2.1816	400	0.0043	0.0008	0.1810	1
	2.2092	400	0.0044	0.0010	0.2179	2
	2.1742	400	0.0043	0.0012	0.2702	3
	2.2373	400	0.0045	0.0020	0.4391	6
	2.1560	400	0.0043	0.0025	0.5750	12
	2.2437	400	0.0045	0.0028	0.6304	60
	1.0133	200	0.0020	0.0016	0.7859	360
	Starting Mass(gms)	Volume (mLs)	$Hg_{Initial}$	Hg_{Final}(avg.)	Conversion ($Hg_{Final}/Hg_{Initial}$)	Time (minutes)
Mercury	2.1816	400	0.0097	0.0009	0.0941	1
	2.2092	400	0.0099	0.0020	0.2010	2
	2.1742	400	0.0097	0.0029	0.2966	3
	2.2373	400	0.0100	0.0068	0.6775	6
	2.1560	400	0.0096	0.0089	0.9235	12
	2.2437	400	0.0100	0.0106	1.0593	60
	1.0133	200	0.0045	0.0047	1.0355	360
	Starting Mass(gms)	Volume (mLs)	$Si_{Initial}$	Si_{Final}(avg.)	Conversion ($Si_{Final}/Si_{Initial}$)	Time (minutes)
Silicon	2.1816	400	0.0006	0.0001	0.1271	1
	2.2092	400	0.0006	0.0001	0.1477	2
	2.1742	400	0.0006	0.0001	0.2302	3
	2.2373	400	0.0006	0.0001	0.2403	6
	2.1560	400	0.0006	0.0002	0.4243	12
	2.2437	400	0.0006	0.0002	0.3761	60
	1.0133	200	0.0003	0.0004	1.4501	360
	Starting Mass(gms)	Volume (mLs)	$Na_{Initial}$	Na_{Final}(avg.)	Conversion ($Na_{Final}/Na_{Initial}$)	Time (minutes)
Sodium	2.1816	400	0.0423	0.0137	0.3232	1
	2.2092	400	0.0429	0.0193	0.4508	2
	2.1742	400	0.0422	0.0238	0.5652	3
	2.2373	400	0.0434	0.0354	0.8165	6
	2.1560	400	0.0418	0.0386	0.9238	12
	2.2437	400	0.0435	0.0404	0.9281	60
	1.0133	200	0.0197	0.0197	1.0031	360